Optimal Coordination of Electric Vehicles and Distributed Generators for Voltage Unbalance and Neutral Current Compensation

Md. Rabiul Islam, *Student Member, IEEE,* Haiyan Lu, *Senior Member, IEEE,* M. J. Hossain, *Senior Member, IEEE,* Li Li, *Member, IEEE*

***Abstract*— To maximize renewable energy usage to combat climate change, the penetration of electric vehicles (EVs) has increased significantly in developed countries. This can cause serious power quality issues, such as increased voltage imbalance and neutral currents, which severely impact the operation of power systems. Although the power quality issue is not a new problem, it requires an improved strategy for the growing penetration of photovoltaic (PV) solar energy and electric vehicles in low-voltage distribution grids and their uncoordinated operation. This paper presents a new control strategy to reduce the number of coordinated EVs to mitigate voltage unbalance and compensate for the neutral current. The proposed control strategy consists of two controllers arranged in a hierarchical structure with the central controller at the top layer and the local controller at the bottom layer. The central controller is in charge of two control processes: one is the primary control operated jointly by distribution network operators (DNOs) and PV owners to coordinate the phases and optimal dispatch of distributed PV solar plant; another is to coordinate an optimum number of EVs at the sensitive bus in the secondary control by accounting for the proposed local controller (three-phase four-leg EV converter) capacity. It is evident that the proposed control strategy reduces the number of EVs that need to be coordinated, and further, EV coordination is not required if the grid imbalance is less. This new hierarchical control strategy can improve power quality and reduce data processing overhead and computational complexity.**

***Index Terms*— heirarchical control, neutral current, voltage unbalance, EV coordinating, EV converter.**

I. Introduction

Due to the growing penetration of electric vehicles (EVs) and photovoltaic (PV) solar plants into distribution grids, distribution network operators (DNOs) are facing significant challenges in maintaining power quality. The power quality problem includes voltage drop and grid imbalance (voltage unbalance, and larger neutral current) for a low voltage (LV) distribution grid. Both EV charging loads and distributed generation (DG) units induce imbalance into the distribution grid. The increased capacity of DG units' size increases imbalance if they are randomly distributed among nodes [1]. The voltage unbalance factor (VUF) increases with an increased PV size if they are uncoordinated between phases in a distribution grid [2]. The balance between demand-generation is not only important for pricing [3] but also for balancing the distribution grid [2]. The work in [4] showed that the time-varying load, location and size of the PV units and their penetration has a higher impact on the VUF of a distribution grid in Spain. Therefore, both EV and PV integration in a LV distribution grid can increase grid imbalance [5]. Grid imbalance is harmful for inductive loads, transformers, and electronic devices [6]. It also increases operation costs, neutral conductor sizes [7], [8] and decreases the voltage at different nodes [5], [9].

Regarding power quality, two of the most commonly used indices to measure grid imbalance are the VUF and the neutral current. These two indices are influenced by active and reactive power through the direct injection or adjusting level of the load balance. In the literature, several control methods have been proposed to compensate for voltage imbalance and/or reduce the neutral current by controlling single phase or three-phase PVs and EVs. To the author's best knowledge, only a few control approaches have been proposed to compensate for voltage unbalance by coordinating single phase PVs and EVs [2],[10]- [13]. In [2], additional active power from a battery energy storage (BES) with a PV unit was injected to compensate for voltage unbalance between phases. Each single-phase residential customer [10] and EVs [11] require a dynamic switch which can transfer load or EV charging demand from one phase to another phase in a three-phase distribution grid to mitigate voltage unbalance. In [11], EVs were not only switched from one phase to another phase but also each EV charging or discharging active power is controlled to compensate for voltage unbalance. The reactive power support from a PV unit through custom power devices such as a dynamic voltage restorer (DVR) and a dynamic static compensator (DSTATCOM) was proposed to compensate for voltage unbalance in [12]. Both active and reactive power support from EVs was controlled to compensate for voltage unbalance and to improve voltage in [13].

In addition to a single-phase PV and EV unit, recently, some control approaches have been proposed to control three-phase PV and EV converters to compensate for voltage unbalance [14]-[18] and neutral current [19]. The

Manuscript received XXXX; revised XXXX; accepted XXXX. Paper XXXXX, approved for publication in the IEEE TRANSACTIONS ON INDUSTRY APPLICATIONS by the XXX committee. This research is supported by an Australian Government Research Training Program.

M. R. Islam, H. Lu, M.J. Hossain, and Li. Li are with the Faculty of Engineering and Information Technology, University of Technology Sydney, Broadway, New South Wales 2007, Australia, (e-mails: mdrabiul.islam-1@student.uts.edu.au;haiyan.lu@uts.edu.au; jahangir.hossain@uts.edu.au; li.li@uts.edu.au).

Color versions of one or more of the figures in this paper are available online at http://ieeexplore.ieee.org.
Digital Object Identifier XXX/TIA.XXX

three-phase EV converter injected different amounts of reactive power into different phases (phase a/phase b/phase c) to maintain voltage unbalance [14]. By considering detriment of reactive power compensation, both the PV and EV converter consumed or injected active power into different phases to maintain voltage unbalance between the phases [15]. In addition to injecting either active or reactive power into the three-phases, another commonly used control method for a three-phase PV inverter controls the positive sequence current [16]-[18]. The authors in [7] showed that an active power filter can compensate for a neutral current. Our previous work proposed a PV converter with an active power filtering process to compensate for a neutral current in [19]. The aforementioned control methods for PV inverters require an intricate control strategy due to the intermittent nature of solar energy. Although these control methods are promising to a certain extent, they have the following limitations:

- These control methods coordinate all EVs and PVs in the LV distribution network and require a large amount of data processing and also increase computational complexity.
- The reactive power compensation requires additional inverter capacity [20], [21] and grid constraints are also a limiting factor for existing reactive power compensation methods.
- Some control methods [10], [11] require a large number of EV switching between phases with a growing number of EVs.
- These control methods only deal with either voltage unbalance or a neutral current. But both imbalance indices (voltage unbalance and neutral current) degrade grid performance.
- These control methods were not evaluated by addressing the different amount of grid imbalance.

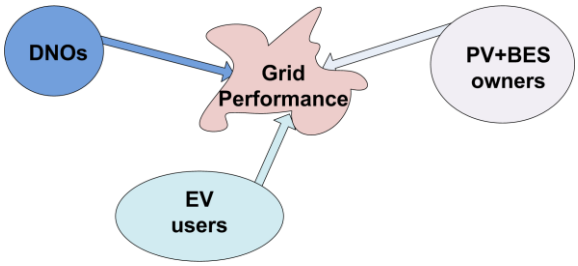

Fig. 1. Proposed participants to improve grid performance

This paper aims to improve power quality by minimizing both voltage unbalance and neutral current by solving a multi-objective optimization problem. In [9], the weighted sum optimization method with multiple objectives was used. The weighted sum optimization approach does not guarantee to compensate for maximal voltage unbalance and minimal neutral current simultaneously by considering a different amount of grid imbalance. Therefore, an improved control strategy is required to minimize both indices subject to complex constraints.

This study proposes a new control strategy with a hierarchical structure to minimize both voltage unbalance and neutral current. This control strategy consists of two controllers arranged in a hierarchical structure with the central controller at the top layer and the local controller at the lower layer. Three stakeholders (DNOs, PV owners, and EV users) are involved in this coordination, as shown in Fig.1. The central controller controls and communicates with the DNOs and PV owners at the primary control layer. If the desired performance is not achieved, EVs of the sensitive nodes or buses are controlled at the secondary control layer. If further improvement is required, the proposed three-phase EV converter is assigned as the local controller based on its ability to compensate for grid imbalance. In other words, the central controller optimizes the number of EV participants to achieve the highly prioritized objective (voltage unbalance) whereas a less prioritized objective is compensated for using a local controller (EV converter). In summary, the key contributions of this paper are to:

- develop a hierarchical control strategy with a central controller in charge of primary and secondary controls to optimally dispatch PVs and EVs;
- design and implement a smart local controller that consists of an improved three-phase four-leg EV converter to enhance the neutral current compensation capability; and
- develop a central control method using the power quality issues in sensitive buses and a smart local controller capability to reduce the number of contributing EVs in coordination to support the distribution grid.

The proposed hierarchical control strategy provides greater flexibility to include PV owners and EV users as contributors to compensate for voltage unbalance and neutral current irrespective of the extent of grid imbalance. This strategy not only compensates for voltage unbalance and neutral current, it also requires a smaller number of PV owners and EV users as contributors to support the distribution grid. It also does not require information from all the active EVs (e.g., charging or discharging power, SoC rate) at each timeslot and this reduces the volume of data to be processed and the computational burden.

The rest of the paper is organized as follows: Section II explains the control objectives and Section III presents the hierarchical control strategy. Section IV details the experimental system. Section V presents the evaluation of the control strategy based on the experiment results. Section VI draws the conclusions and provides suggestions for future work.

II. Control Objectives

Given an LV distribution network, the proposed control strategy aims to achieve minimal voltage unbalance and neutral current by the optimal coordination of PV dispatch and EV charging and discharging with multiple control layers. This section defines the control objectives.

This study considers two of the most commonly used grid imbalance indices: voltage unbalance factor (VUF) which is used to indicate the degree of voltage unbalance during power flow computation, and the neutral current (I_n).

A. Determination of the voltage unbalance factor (VUF)

The VUF at a node of a distribution grid indicates the degree of imbalance due to the connected distributed generation sources and load distribution between phases. The value of the VUF at every measuring node must be below 2-3% [8]. The VUF at node *mv* at time step *t* is defined in this study according to IEEE standard 1159 [22].

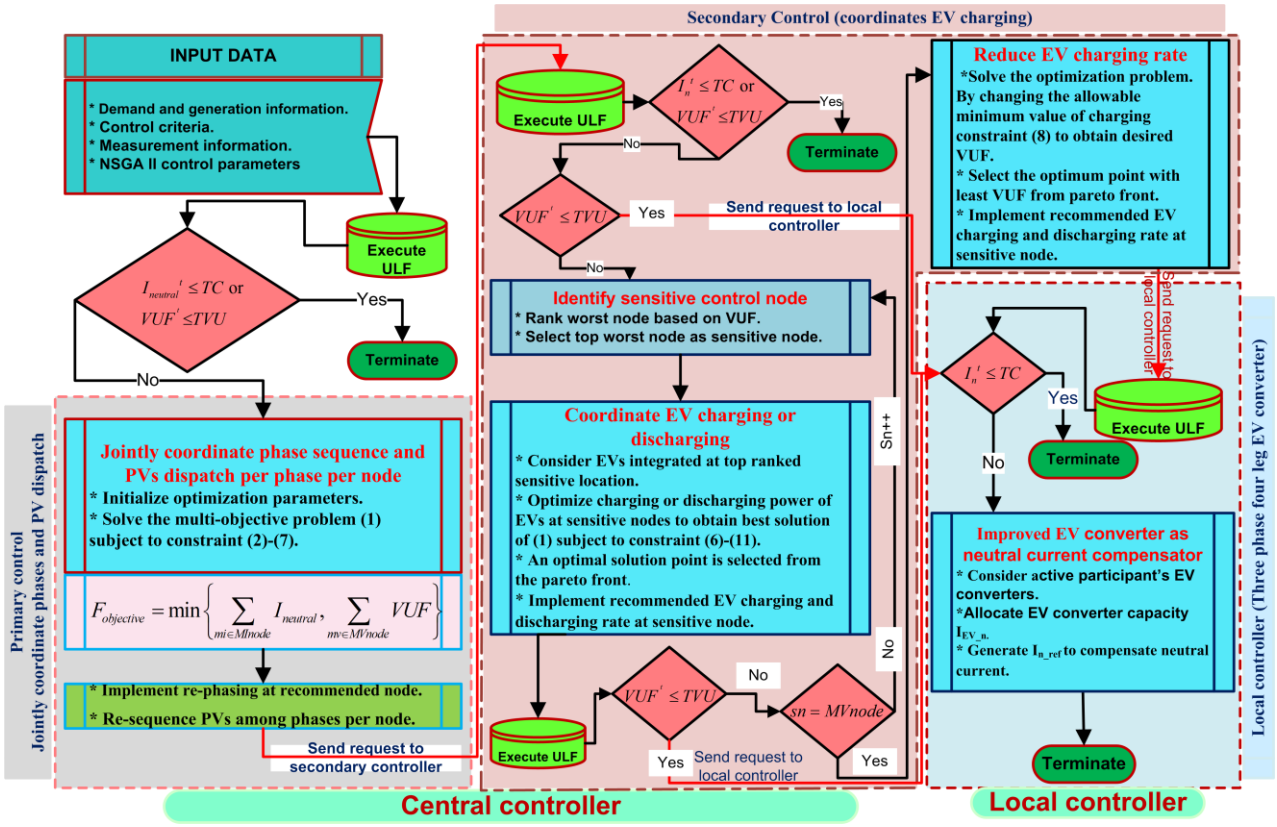

Fig. 2. Flow chart of the proposed hierarchical control method

B. *Determination of neutral current ($I_{neutral}$)*

Every three-phase unsymmetrical system of phasors consists of the three symmetrical systems of zero, positive and negative sequences according to the Stokvis-Fortescue theorem [23]. The neutral current ($I_{neutral}$) is the summation of the three-phase current at a current measuring node (mi).

C. *Control objectives*

Suppose in a given LV network, the total number of voltage measuring nodes is MVnode and the total number of neutral current measuring nodes is MInode, and there are T control steps (24h in a day).To compensate for voltage unbalance and neutral current at all the respective measurement nodes, the control objective function $F_{objective}$ is expressed as:

$$F_{objective} = \min \begin{cases} \sum_{mi \in MInode} I_{neutral}^{mi} \\ \sum_{mv \in MVnode} VUF^{mv} \end{cases} \quad (1)$$

where mv is the VUF measuring node and considers all the voltage measuring nodes (MVnode), mi is the neutral current measuring node and considers all the current measuring nodes (MInode).

III. Control Strategy

Each Each distribution grid has a certain grid performance standard. In this study, the Australian standard is used as the control constraints for a distribution grid. Under this standard, the distribution network has two control conditions, (TC and TVU) which must be satisfied, where TC is the threshold of the neutral current at a measuring node (*mi*) and TVU is the threshold of VUF at a measuring node (*mv*) in a distribution grid. These control conditions are checked at each time step (t) of a day after the measurement information has been received. The control objective (1) is maintained through using the proposed hierarchical control strategy. This proposed control strategy has a hierarchical structure which includes a central control layer and a local control layer. The central controller performs the following two tasks:

i) Primary control: to simultaneously balances the phases and PV power dispatch.

ii) Secondary control: to coordinate EV charging and discharging.

The local controller measures the neutral current at a node and is triggered if the neutral current is above the threshold after receiving instructions from the central controller.

The flow chart of this hierarchical control strategy, including the three controller blocks, is shown in Fig. 2. The central controller evaluates the control criteria (VUF and neutral current). If the VUF and the neutral current are greater than the threshold, the primary control method jointly balances the phases and the PV dispatch. After implementing the primary control method, the control criteria are re-evaluated. If the control criteria are not achieved, the central controller performs either secondary control if VUF is greater than the threshold or requests the local controller if the neutral current is above the threshold. In the secondary control method, EVs are coordinated at the recommended sensitive nodes with an optimum charging rate. Both controllers are described in the next sub-section.

A. *Central Controller*

The central controller performs the primary and secondary control method. The primary control method uses DNOs and the PV owner's resources whereas the secondary control method coordinates EV charging. Both the primary and secondary control methods are described below:

1) Primary Control (Jointly Coordinate Phases and PV Dispatch)

The central controller includes DNOs as a primary contributor and recommends the phase selector switch is installed at each node. The phase selector switch has the ability to change a phase sequence from (A,B,C,N) to either (B,C,A,N) or (C,A,B,N). In this study, three-phase sequences (A,B,C,N), (C,A,B,N), and (B,C,A,N) are represented as 0,1,and 2. Furthermore, the central controller includes PV owners (installed with BES) in the control process. The recommended single phase PV owners (installed with BES) are asked to install a switch box which has the ability to switch from phase A to either phase B or phase C. These switches are installed with a ZigBee wireless receiver to receive control information, and are designed with TRIAC, a snubber circuit, and over-voltage protection [24]. These switches are the re-sequencing phases after receiving the control information from the central controller as shown in Fig.3.

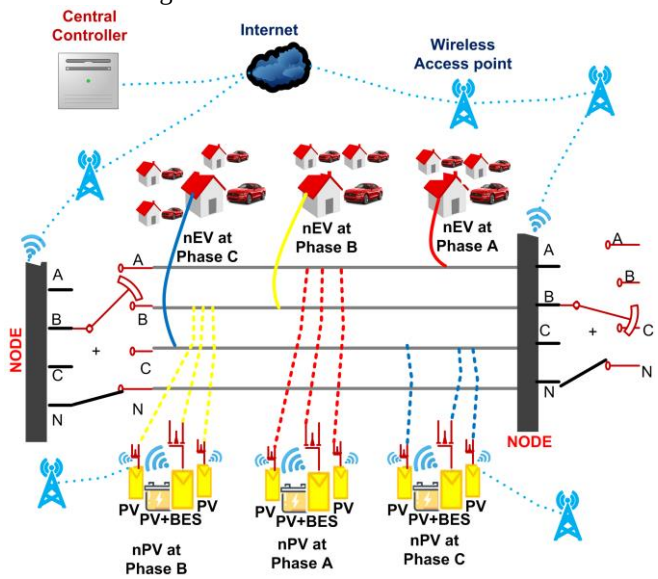

Fig. 3. Proposed primary control method

Both contributors (DNOs and PVs) jointly participate in the execution of the primary control method. In the primary control, the central controller collects measurement information such as the lump sum of demand (residential and EV charging) and generation per phase per node, node voltage, VUF, neutral current at the measurement nodes, and the amount of PV output power between phases of the contributing PV plants at a time step. It also checks the control conditions at each time step and performs the primary control method if the constraints are violated. The central controller controls both node and PV switches to achieve minimal voltage imbalance and neutral current by solving the following multi-objective optimization problem (1) subject to:

$$P(\kappa,t)_{PV\_BES\_min} \le P(\kappa,t)_{PV\_BES} \le P(\kappa,t)_{PV\_BES\_max} \quad (2)$$

$$\sum_{\delta \in nPV} P(\delta,t)_{PV} + \sum_{\kappa \in nBES} P(\kappa,t)_{PV\_BES} = Y \quad (3)$$

$$\sum_{\Omega \in NRES} P(\Omega,t)_{res} = U, \sum_{\nu \in NEV_c} P(\nu,t)_{EV\_ch} = V \quad (4)$$

$$\sum_{\mu \in nEV_d} P(\mu,t)_{EV\_dch} = Z \quad (5)$$

$$P(Br,t)_{loss} = \sum_{Br \in Nbranch} R(Br,t) \times \left| I(Br,t) \right|^2 \quad (6)$$

$$0.95 \text{ p.u} \le V(t)^m \le 1.05 \text{ p.u} \quad (7)$$

where Y, Z, U, and V are constants whose values remain unchanged before and after control. κ belongs to all PV plant installed with BES, δ belongs to all PV plant without BES, Ω belongs to all residential loads, ν belongs to all charging EVs, μ belongs to all discharging EVs, and Br belongs to all branches in a distribution grid.

In a distribution grid, single-phase and three-phase PVs can feed power into the grid, but the PV owners are only paid for the fed-in active power. For this reason, reactive power support from the PV is not considered in this study. The integration of a single phase PV in a distribution grid may increase grid imbalance and energy loss [5] if the PV's dispatch is not coordinated in real- time [25]. In this study, it is considered that a single-phase PV plant is installed with or without BES. In this study, the effect of solar irradiance, solar cells and converter efficiency are not considered in PV power modelling. The converter output of a PV plant (installed without BES) is considered at time step (t). The output of a PV plant (installed with BES) can be made dispatchable by controlling the respective BES's discharging rate (2). The proposed control strategy recommends the optimum PV (installed with BES) power at the respective phase. The amount of delivered single-phase PV power (installed with BES) between the phases is controlled by a phase selector switch. In this study, the total amount of delivered single phase PV and BES power per node remains the same at a time step. The total power generation from PV (P_{pv}), and battery energy storage (P_{BES}), remains unchanged before and after control, as shown in (3). The total residential demand (P_{RES}), electric vehicle charging demand (P_{EV_ch}), and EV dispatched power (P_{EV_dch}) of a distribution grid remain the same as shown in (4)-(5). The total energy loss is the lump sum of all branch loss as given in (6). The voltage should be regulated between 0.95 p.u to 1.05 p.u as shown in (7) according to the Australian standard [8].

2) Secondary Control (Coordinates EV Charging)

After performing the primary control method, the central controller re-evaluates the network performance and checks the control conditions. If the value of VUF is below the standard value (2%) but the neutral current is above the threshold, the local controller is triggered to compensate for the neutral current at the respective measuring point. If the value of VUF is still not achieved, the central controller ranks nodes based on the value of VUF. The central controller collects information on the EV charging and discharging rate at the sensitive node. The EV charging and discharging rate is optimized by solving a multi-objective optimization problem shown in (1) subject to:

$$P(\nu,t)^{sn}_{EV\_ch\_min} \le P(\nu,t)^{sn}_{EV\_ch} \le P(\nu,t)^{sn}_{EV\_ch\_max} \quad (8)$$

$$P(\mu,t)^{sn}_{EV\_dch\_min} \le P(\mu,t)^{sn}_{EV\_dch} \le P(\mu,t)^{sn}_{EV\_dch\_max} \quad (9)$$

$$P(\nu,t)_{EV\_ch}^{Nsn} = W, P(\mu,t)_{EV\_dch}^{Nsn} = T \tag{10}$$

$$\sum_{\delta \in nPV} P(\delta,t)_{PV} + \sum_{\kappa \in nBES} P(\kappa,t)_{PV\_BES} = Y, \sum_{\Omega \in NRES} P(\Omega,t)_{res} = U \tag{11}$$

where the sum of sensitive (sn) and non-sensitive nodes (Nsn) is equal to the total nodes ($sn + Nsn = MVnode$), and T, Y, and U are constants whose values remain unchanged before and after control.

A method of using the variable EV charging and discharging rate is applied in this study whereas the EV charging and discharging rate is limited within its minimum (P_{d/ch_min}) and maximum (P_{d/ch_max}) limit as shown in (8)-(9). The EV charging or discharging rate at the non-sensitive nodes (Nsn) remains the same as shown in (10). The secondary control method ranks nodes based on VUF value. Nodes are ranked in descending order and the top ranked node is considered to be a sensitive node. The EV charging and discharging rate is controlled at the sensitive nodes (sn) whereas the total residential demand, PV and BES output power remain unchanged as shown in (11). The EVs at the sensitive nodes are repeatedly ranked and optimized until the VUF value satisfies the control constraints with the least neutral current.

The total number of sensitive nodes depends on the degree of grid imbalance in a distribution grid. The increasing number of sensitive nodes means more EV are participating which increases the number of coordinated EVs until the desired VUF value is achieved or all EVs are included (including all nodes as sensitive nodes (MVnode)). The proposed secondary control method solves the problem (1) using the NSGA II optimization algorithm. The NSGA II recommends a set of solutions through its Pareto front. From the Pareto front, an optimal solution is chosen by prioritizing VUF. The less prioritized objective (the neutral current) is compensated for through the local controller if the neutral current is below the threshold (TC) at the respective measurement point.

B. Local Controller

This local controller measures the neutral current at a node and is triggered if the neutral current is above the threshold (TC) after instructions from the central controller have been received. The amount of current required to compensate for the neutral current depends on the EV converter's capacity. Usually, the active and reactive power is controlled using a traditional three-phase three-leg EV converter. The four-leg controller is designed to compensate for the neutral current based on the available EV converter's capacity. The EV converter's apparent capacity can be expressed as (12).

$$S_{EV} = \sqrt{U_{EV\_n}^2 + \left(P_{EV}^2 + Q_{EV}^2\right)} \tag{12}$$

where P_{EV} denotes active power and Q_{EV} denotes reactive power in a three-phase three-leg EV converter, and U_{EV_n} denotes the EV converter's capacity in the improved controller with four-leg. This capacity also limits the neutral current compensation ability of a local controller.

The configuration of this new four-leg EV converter connected at a node in a distribution grid is shown in Fig. 4. The single-phase equivalence of a three-phase four-leg converter is described in [26]. The mathematical presentation (in a synchronous rotating frame) of the designed EV three-phase four-leg converter is shown in Figure 4 [26]:

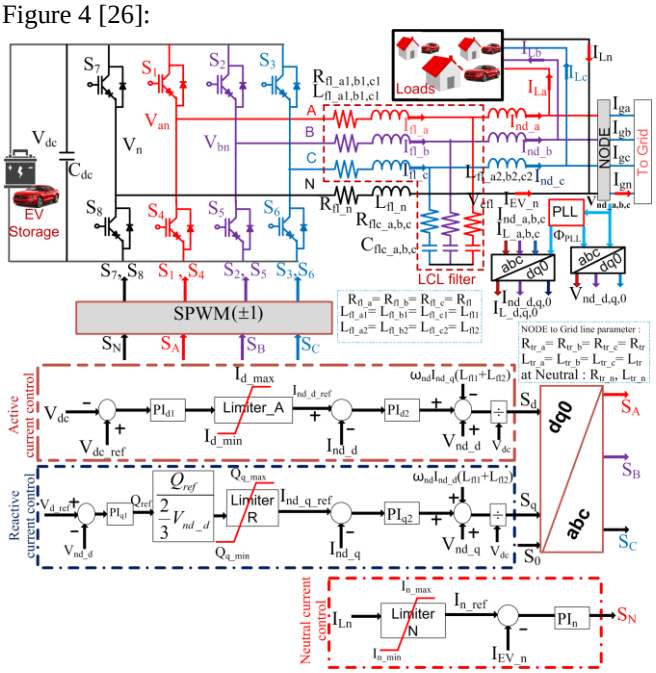

Fig. 4. Proposed local controller

$$\frac{d}{dt} I_{fl(d,q)} = \frac{V_{dc}}{L_{fl1}} - \frac{R_{fl}}{L_{fl1}} I_{fl(d,q)} - \frac{R_{flc}}{L_{fl1}} \left(I_{fl(d,q)} - I_{nd(d,q)} \right) - \frac{V_{cfl(d,q)}}{L_{f1}} \pm \omega I_{fl(q,d)} \tag{13}$$

$$\frac{d}{dt} I_{nd(d,q)} = \frac{V_{cfl(d,q)}}{L_{tr}} - \frac{R_{tr}}{L_{tr}} I_{nd(d,q)} + \frac{R_{flc}}{L_{tr}} \left(I_{fl(d,q)} - I_{nd(d,q)} \right) - \frac{V_{nd(d,q)}}{L_{tr}} \pm \omega I_{nd(q,d)} \tag{14}$$

$$\frac{d}{dt} V_{cfl(d,q)} = \frac{I_{fl(d,q)}}{C_{flc}} - \frac{I_{nd(d,q)}}{C_{flc}} \pm \omega V_{cfl(q,d)} \tag{15}$$

$$\frac{d}{dt} V_{dc} = \frac{I_{EV}}{C_{dc}} - \frac{\sum I_{fl(d,q,0)} d_{d,q,0}}{C_{dc}} \tag{16}$$

$$\frac{d}{dt} I_{fl(0)} = \frac{1}{L_{fl1} + 3L_{fl\_n}} V_{dc} d_0 - \frac{R_{flc} + 3R_{fl\_n}}{L_{fl1} + 3L_{fl\_n}} I_{fl(0)} - \frac{R_{flc}}{L_{fl1} + 3L_{fl\_n}} \left(I_{fl(0)} - I_{nd(0)} \right) - \frac{V_{cfl(0)}}{L_{fl1} + 3L_{fl\_n}} \tag{17}$$

$$\frac{d}{dt} I_{nd(0)} = \frac{1}{L_{tr} + 3L_{tr\_n}} V_{cfl(0)} - \frac{R_{tr} + 3R_{tr\_n}}{L_{tr} + 3L_{tr\_n}} I_{nd(0)} + \frac{R_{flc}}{L_{tr} + 3L_{tr\_n}} \left(I_{fl(0)} - I_{nd(0)} \right) - \frac{V_{nd(0)}}{L_{tr} + 3L_{tr\_n}} \tag{18}$$

$$\frac{d}{dt} V_{cfl(0)} = \frac{I_{fl(0)}}{C_{flc}} - \frac{I_{nd(0)}}{C_{flc}} \tag{19}$$

$$I_{EV\_n} = -3I_{fl(0)} \tag{20}$$

where the quantities with the subscripts 'fl' , 'nd' , and 'tr' denote the EV converter filter side, node side, and distribution lines respectively, and the other symbols bear their usual meaning. The actual ac quantity (a,b,c) is transformed to dc quantity (d,q) using the synchronous rotating frame theory as shown in (13)-(20) to investigate the relationship between d,q, and zero sequence components in our study. The relationship between the neutral current and zero sequence component is shown in (20), which

means that controlling any one component has a direct impact on another. Another advantage is that both components have no coupling terms with the d and q components as shown in (13)-(20). Therefore, the neutral current compensation method can be employed with the active and reactive power control method, respectively. In this study, the contributing three-phase EV converters are used to compensate for the neutral current whereas the designed converter can perform active and reactive power control tasks. The individual control blocks are shown in Fig.4 where the reference neutral current is controlled via the central controller. The neutral current (I_{Ln}) after optimization is a direct reference neutral current which is sent to the local controller via the central controller. The local controller sends the required capacity information to the EV converter and the EV converter allocates the EV capacity within its boundary (12). The saturation limiter has minimum (I_{n_min}) and maximum (I_{n_max}) values. The minimum value (I_{n_min}) is equal to the threshold value of the neutral current. The amount of compensated neutral current is limited to the maximum EV converter's capacity (I_{n_max}) at a time step. Any remaining capacity after neutral current compensation can be used for active and reactive power control. The control blocks and the sinusoidal pulse width modulation (SPWM) is shown in Fig.4.

IV. Experimental System and Design

In order to evaluate the proposed hierarchical control strategy, an experimental system is designed and simulated using the DIgSILENT Power Factory software package [27]. The average hourly residential load data and distribution grid model are obtained from a distribution grid operator in Queensland, Australia. The distribution grid is shown in Fig.5. To investigate the efficacy of the proposed control strategy, reactive power compensation equipment is not considered in this study. EV loads are imposed on the distribution grid, assuming each resident (725 households) has an EV and is connected to the distribution grid either in charging or discharging mode. When EVs are not connected to the distribution grid, they are not in service and are not included in the control strategy. In the control strategy, single phase EVs with different charger ratings (3.8 kW, 4.8 kW, 5.8 kW, 7.7 kW, 9.6 kW, 11.5 kW, and 15.4 kW) are coordinated by controlling the charging and discharging rate. Each EV acts as a constant load with a unity power factor during charging until reaching a desired SOC. The EV acts as a distributed generation source with a unity power factor during discharging until reaching an allowable minimum SOC. The VUF is measured at each node and nodes #M04, #M06, #M08, and #M12 are considered as the neutral current measurement nodes, as shown in Fig. 5. Local controllers (three-phase four-leg EV converter) are connected at nodes #M04, #M06, #M08, and #M12. In the three-phase four-leg converter, the DC capacitor is tuned at 5000μF, LCL filter parameter is 5mH and 10μF, and the switching frequency is tuned at 2.5 kHz.

The degree of imbalance in a distribution grid, denoted by ξ, depends on the EV and PV distribution between phases. The work in [28] shows that uncertainty in the EV travel schedule, failure of the charging equipment, scheduling errors etc. can cause load imbalance between phases and has a severe impact on grid performance [5]. Grid imbalance may occur due to EV uncertainty, although total demand is

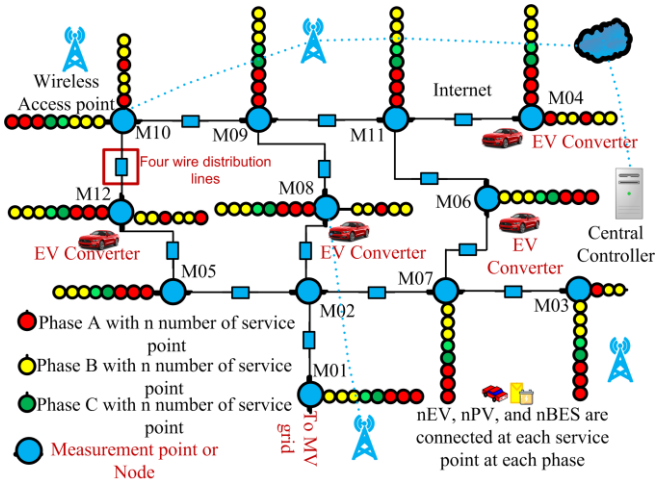

Fig. 5. Test distribution grid

equal to scheduled demand. To investigate the impact of phase imbalance on the distribution grid, EVs are distributed unequally between phases (P_A, P_B, P_C) according to (21) without changing the total EV charging demand. The degree of grid imbalance (ξ) is defined as the percentage of total load changes between phases, as expressed in (21). $P_{\{A,bal\}}$, $P_{\{B.bal\}}$, $P_{\{C,bal\}}$ is the load connected to respective phase in the balanced system. When the value of ξ is 0%, this means that the loads are balanced between the three phases. The degree of imbalance ξ is increased by transferring a portion of load from two phases (phase A and phase B) to another phase (phase C). When ξ is 100%, all the loads are connected to phase C by keeping the total EV charging demand the same.

$$\begin{aligned} P_A &= P_{\{A,bal\}} - \xi \\ P_B &= P_{\{B,bal\}} - \xi \\ P_C &= P_{\{C,bal\}} + 2\times\xi \end{aligned} \tag{21}$$

where $\xi = \%of\ \frac{P_{total}}{3}$, $P_{total} = \sum_{\alpha=A,B,C} P_{\{\alpha,bal\}}$

Using this system, the following scenarios are evaluated:

- Scenario I (Uncoordinated method): Investigate the impact of the degree of grid imbalance (ξ) on a distribution grid's performance.
- Scenario II (Proposed control method): Investigate the efficacy of the proposed hierarchical control strategy in a number of cases with an imbalance degree ranging from 5% to 100%.

V. Results and Discussion

This section presents the obtained results to evaluate the proposed control strategy and the efficacy of the proposed control strategy is compared with the recent research works on mitigating VUF and compensating for the neutral current.

A. *Uncoordinated Method*

In this study, the impact of grid imbalance (ξ) on distribution grid performance is investigated at 14:00 hours of a day by varying imbalance ξ. The load flow diverges when the degree of imbalance (ξ) increases to over 50% due to branch and grid capacity constraints. The impact of grid imbalance (scenario I) on the distribution grid is shown in Fig. 6. The following observations are made from Fig. 6:

- The VUF of the distribution grid increases with increasing grid imbalance (ξ), as shown in Fig. 6(a).

- The neutral currents at the measurement nodes are summed and presented in Fig. 6(b), which shows that increased imbalance produces a higher amount of neutral current.
- Energy loss is also increasing due to imbalance, as shown in Fig. 6(c), and
- The voltage unbalance at each node is increasing with the amount of imbalance (ξ), as shown in Fig. 6(d).

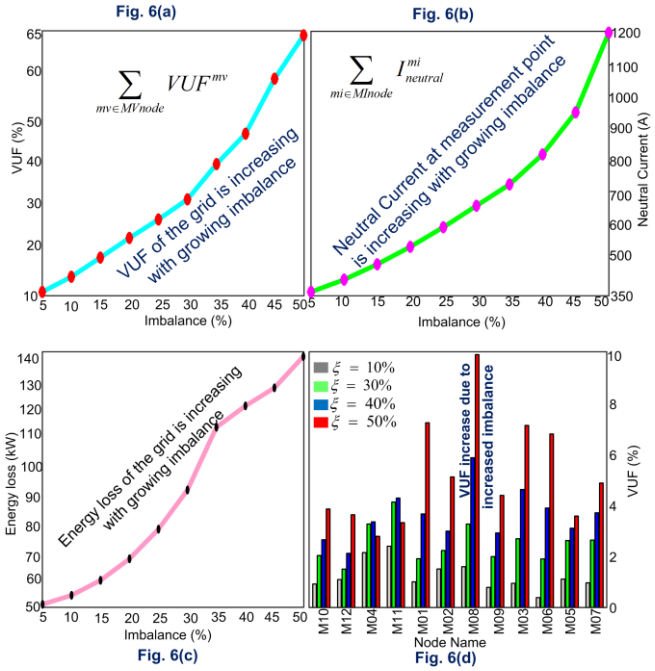

Fig. 6. Impact of grid imbalance (ξ) on distribution grid

TABLE I
PROPOSED PHASE SEQUENCE (IMBALANCE =25%)

Node name	Proposed phase sequence	Node name	Proposed phase sequence
M10	2	M08	1
M12	0	M09	2
M04	0	M03	2
M11	2	M06	0
M01	1	M05	1
M02	2	M07	0

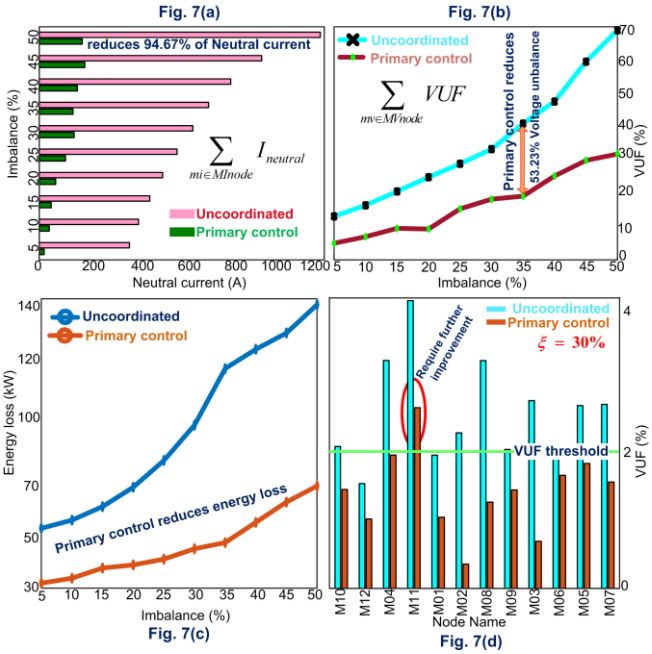

Fig. 7. Impact of primary control method on distribution grid

B. *Central Controller*

1) Primary Control Method

In scenario II, the proposed hierarchical control strategy implements primary control first. At the primary control, DNO and PV contributors are triggered to switch node switches and PV with optimum dispatch to mitigate the impact of grid imbalance. The primary control method is applied at 14:00 hours considering a number of cases with an imbalance degree ranging from 5% to 50%. The node switching re-arrangement in the primary control method is shown in Table I when the grid imbalance (ξ) is 25%. It is assumed that all phases were in the (A, B, C, N) phase sequence before re-sequencing. The primary control method does not recommend re-sequencing phases at node #M12, #M04, #M06, and #M07. The obtained results are compared with uncoordinated performance (scenario I), as shown in Fig. 7. The following observations are made after implementing the primary control method:

- The primary control method compensates for the neutral current by up to 94.68%, as shown in Fig. 7(a).
- The voltage unbalance of the grid reduces up to 62.65% compared to the uncoordinated method, as shown in Fig. 7(b).
- The effect of decreased imbalance saves up to 57.58% of energy, as shown in Fig. 7(c).
- The primary control method cannot reduce VUF to below 2% at each node when the amount of grid imbalance ξ is 30%, as shown in Fig. 7 (d).

The amount of voltage unbalance reduction of a distribution grid using the primary control method depends on the degree of imbalance (ξ).

The primary control method jointly re-sequences PV dispatch and load distribution between phases per node without changing the EV charging rate and PV dispatch as in (3)-(5). These constraints limit the primary control method to achieve the desired VUF and neutral current at a higher degree of imbalance (ξ). However, the benefit of accounting for these constraints are (i) increasing convenience for EV users, and (ii) it does not curtail demand or generation to support the grid to maintain reliability and power quality.

2) Secondary Control Method

For further improvement, the central controller applies the secondary control method. The EV charging and discharging rate of the sensitive nodes are controlled to achieve optimum value of the control objective (1) subject to constraints (6)-(11). The secondary control method is employed when ξ is 30%. The

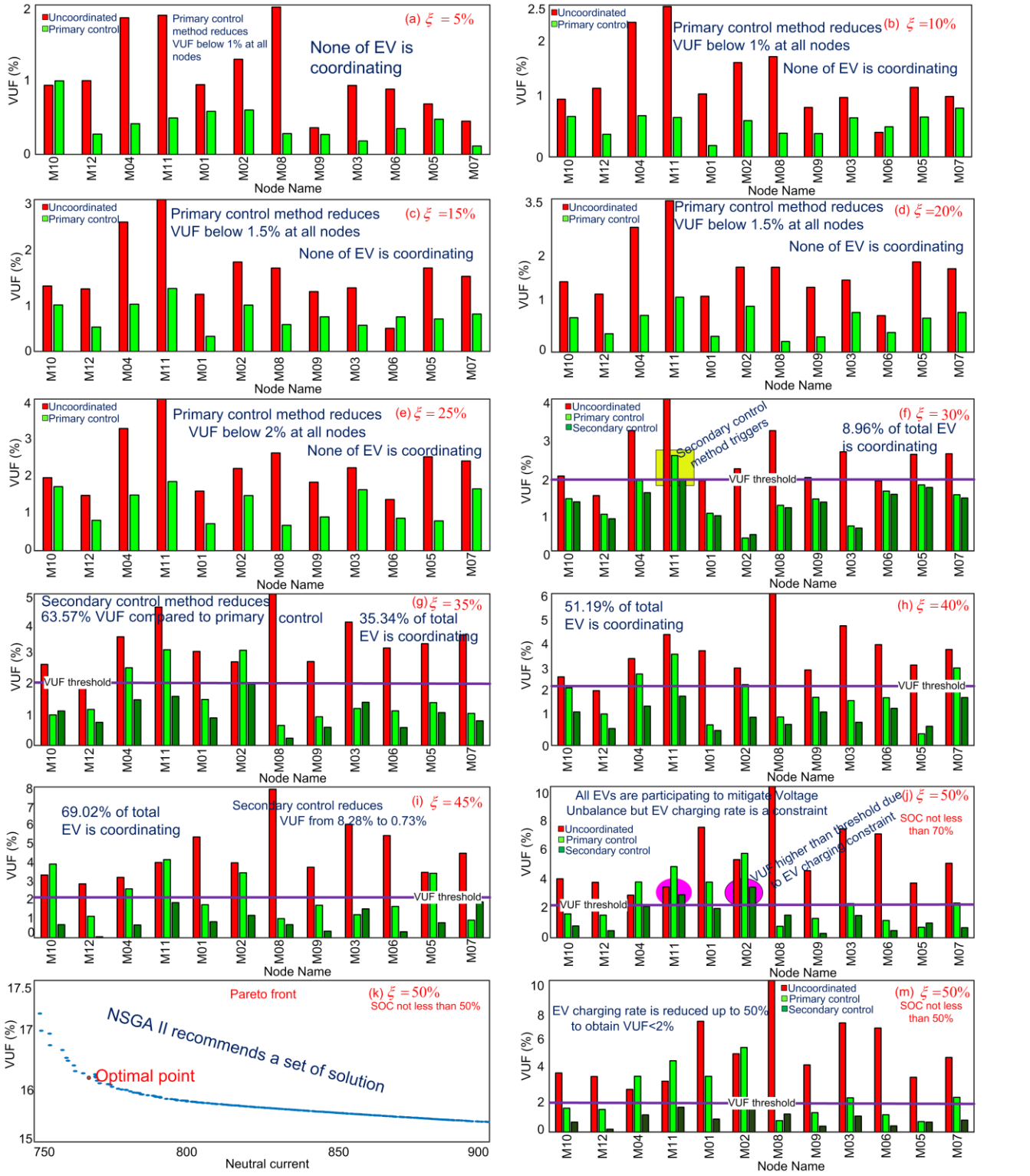

Fig. 8. Impact of central controller on voltage unbalance

node #M11 is considered to be a sensitive node. 8.94% of the total number of EVs connected to node #M11 are controlled through the secondary control method. The secondary control method controls the EV charging rate within a boundary (8) of sensitive node #M11, whereas the charging rate of the rest of the EVs remains unchanged. In this study, the EV charging rate ($P_{EV\_ch\_max}$) can reduce up to 70% in a time step, which is also a constraint (8). In this study, the NSGA II algorithm recommends a set of solutions. The optimal point is selected from the Pareto front with the least VUF and nearer or below the optimum neutral current. The optimum neutral current at a measurement node is equivalent to the available local controller capability at a time step. At 14:00 hours, the available EV converter's capability to compensate for the neutral current is 30 A at node #M08, #M04, neutral current 25A at node #M06, and neutral current 22 A at node #M12. The performance of the central controller after implementing both primary and secondary control is shown in Fig. 8 and Fig. 9. The following observations can be made from Fig. 8 and Fig. 9:

- The primary control reduces the VUF value to below 2% at all nodes until grid imbalance ξ is 25%, as shown in Fig. 8(a)-8(e).

- The central controller triggers the secondary controller when the grid imbalance ξ is 30%, as shown in Fig. 8(f). The secondary control method reduces VUF to below 2% up to the degree of imbalance ξ = 45%, as shown in Fig. 8(f) - Fig. 8(i).
- Due to constraints (6)-(11), the secondary control method cannot reduce VUF to below 2% at all nodes, as shown in Fig. 8(j) in spite of selecting the optimal point from the Pareto front, as shown in Fig. 8(k) when grid imbalance ξ = 50%. It is also seen that a VUF below 2% at all nodes can be achieved by reducing EV charging rate ($P_{EV\_ch\_max}$) up to 50%, as shown in Fig. 8 (m).
- The central controller reduces the neutral current up to 96.48% at node #M08, whereas the neutral current is less than 40A till the grid imbalance ξ=35%, as shown in Fig. 9 (a). The central controller reduces the neutral current to less than 30A at node #M04 and to less than 35 A at node #M12 at grid imbalance ξ=50%, as shown in Fig.9 (c) - Fig.9 (d).

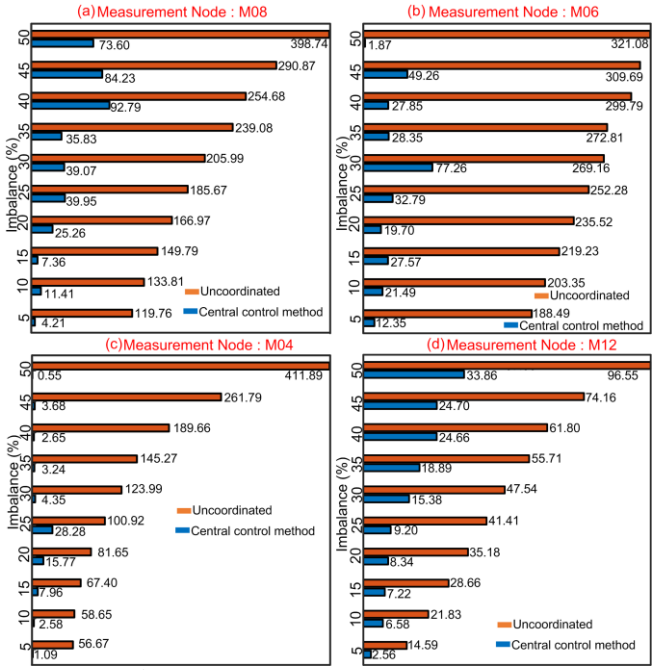

Fig. 9. Impact of central controller on neutral current

C. Local Controller

It is observed from Fig. 9 that there is still a high amount of neutral current which requires further compensation. The central controller sends a requirement about the amount needed to compensate I_{LN} to the local controller at the respective node. The local controller allocates the EV converter's capacity (I_{EV_n}) to compensate for the neutral current to the threshold neutral current value at a measuring node. It is also noted that the required amount of neutral current compensation is not the same for a different degree of imbalance (ξ) at a measurement node. The threshold value of the neutral current is also set by a DNO depending on their grid's capacity (neutral conductor, transformer, etc.). The local controller performance to compensate for a neutral current is shown in Fig 10. The following observations can be made from Fig.10:

- The local controller at node #M08 has a 30A neutral current compensating capability. The central controller reduces the neutral current to 35.83A at node #M08 when the grid imbalance is ξ =35%. The local controller compensates 30A and the rest of the neutral current 5.83 A flows to the distribution grid (I_{gn}), as shown in Fig. 10(a).
- When the grid imbalance ξ is 35%, the local controller is employed after the primary control phase and compensates 25 A at node #M06 and the rest of the neutral current 3.35A flows to the distribution grid (I_{gn}) as shown in Fig. 10(b).
- The local controller can fully compensate the neutral current at node #M04 for all the degrees of grid imbalance (ξ) because the amount of neutral current is below the local controller capability, as shown in Fig. 10(c).
- The central controller reduces the neutral current to 33.86 A when the grid imbalance (ξ) is 50% at node #M12. It is observed from Fig. 10(d) that the local controller can compensate 25 A and allocating additional EV capacity can adequately compensate for the rest of the neutral current.

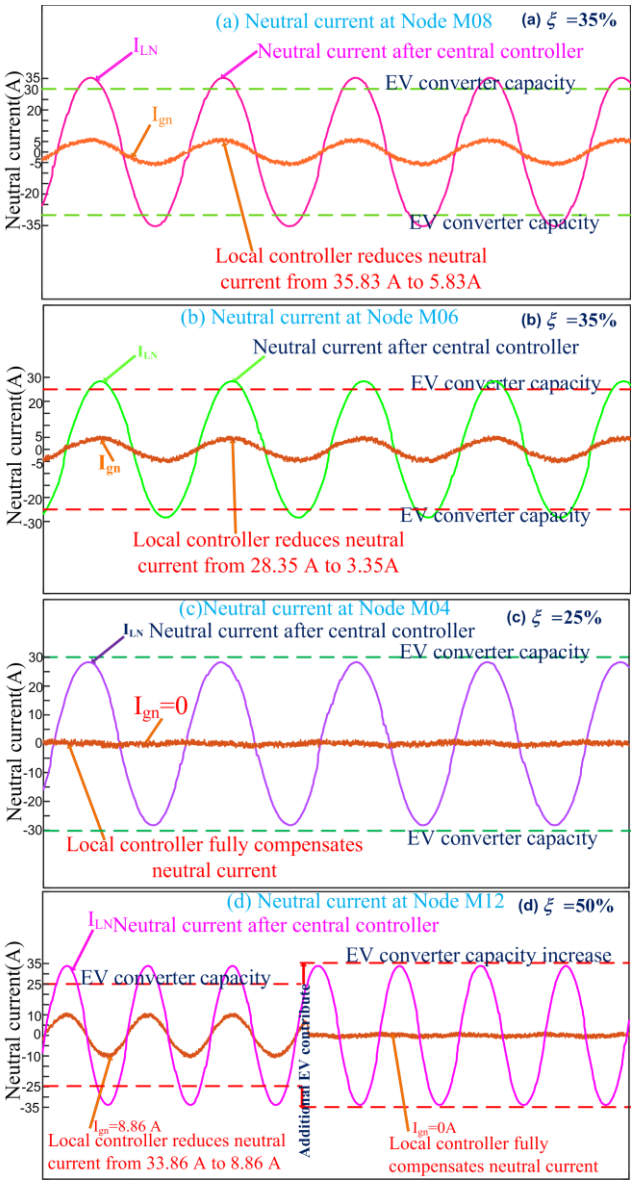

Fig. 10. Impact of local controller on neutral current

The amount of required neutral current compensation depends on DNO, but entirely neutral current compensation improves the power quality. The efficacy of the proposed EV converter shows the robustness of the local controller

method irrespective of the degree of imbalance (ξ) without showing overshoot or significant delay in the output currents.

The computational performance of the proposed control strategy shows that computational time increases with the increasing imbalance of the distribution grid. The primary control method requires computational time up to 45.6 s (when imbalance ξ is 25%) which is implemented on a computer with an Intel Core i7 processor @ 2.80 GHz. The secondary control method recommends the optimal amount of coordinated EVs and computational time increases with the increasing number of coordinated EVs. The central controller requires 109.10 s to coordinate 8.95% of EV whereas 206.67 s is required to coordinate 100% EV of this distribution grid.

Though the proposed hierarchical control strategy improves power quality and computation and execution time, the following challenges should be taken into account during implementation in the power system. The central controller communicates to the re-phasing switches through the Zigbee device. The limitation of the Zigbee device is that it can only cover an extended range of an area of 1.6 km [29]. Therefore, the proposed control strategy is only cost efficient for urban areas. Though the proposed control strategy does not require all the EVs to be coordinated if the voltage imbalance is less, the computational burden increases with the increasing number of coordinated EVs when the degree of imbalance is high. In addition, the proposed control strategy recommends the installation of a three-phase four-leg converter to provide ancillary services. The main challenge is to develop a suitable policy to provide ancillary services to encourage EV owners to install three-phase four-leg converters.

To prove the novelty of this paper, the performance of the proposed method is compared with the recent method proposed in [11] and [30]. Unlike the methodologies for coordinating all EVs in [11], [30] to mitigate voltage unbalance without accounting for the degree of imbalance (ξ), the proposed control strategy decides the number of coordinated EV based on the degree of imbalance (ξ). It is also observed that the primary control method (coordinating phases and PVs) requires less computational time than coordinating all EVs. Coordinating the EV charging method [11], [30] through a variable charging or discharging method reduces the EV charging rate by up to 60% at grid imbalance ξ =25% . On the other hand, the proposed control strategy does not coordinate EVs at grid imbalance ξ =25% which does not reduce the EV charging rate but significantly reduces the computational and execution time. In addition, the novel idea of coordinating EVs at sensitive nodes gives greater flexibility to other EV users connected at non-sensitive nodes. In this way, the proposed control strategy recommends a reduced number of coordinating EVs compared to the variable EV charging method described in [11], [30] as shown in Table II. From Table II, it is observed that coordinating less than 70% of EVs can achieve the desired performance until the degree of imbalance ξ =45%. Furthermore, to ensure there is an optimum number of coordinated EVs with a higher charging rate, the novel idea of employing a local controller is introduced which enhances its capability to compensate for the neutral current. On the other hand, the advantage of using the NSGA II algorithm in this study is that it recommends a set of solutions compromising two objectives (VUF and neutral current) rather than a single solution. Additional support from the local controller (neutral current compensating capability) helps DNOs select an optimum solution point from a set of solutions by giving more importance on VUF than the neutral current. In this way, the proposed hierarchical control method ensures an optimum number of coordinated EVs with a higher charging rate. Hence, the proposed control strategy reduces the number of coordinated EVs, computational time, and communication overhead compared to the recent voltage balancing method [11], [30] by coordinating EVs.

TABLE II
COMPARISON OF EV COORDINATION

The degree of imbalance (ξ) (%)	Proposed control method (% of coordinated EV)	EV charging method [11], [30] (% of coordinated EV)
5%	0%	100%
10%	0%	100%
15%	0%	100%
20%	0%	100%
25%	0%	100%
30%	8.95%	100%
35%	35.34%	100%
40%	51.19%	100%
45%	69.02%	100%
50%	100%	100%

VI. Conclusion

The proposed hierarchical control method allows the participation of DNOs, PVs, and EVs to compensate for neutral current and voltage unbalance by regulating the voltage at each node. Firstly, DNO and PV owners jointly coordinate phases and PV power to improve grid performance. Then, an optimum number of EV users participate in compensating for the neutral current and voltage unbalance if required. The obtained results are presented and compared with the recent balancing method by using real data on an Australian distribution grid. From the obtained results, the following conclusions can be drawn:

i) without optimal coordination of PVs and EVs, an excessive amount of neutral current, voltage unbalance, and energy loss can occur which has a negative impact on a grid's performance;

ii) it is recommended that phases and PVs be coordinated before coordinating EVs to mitigate voltage unbalance and neutral current;

iii) as coordinating a large number of EVs increases the computational burden and communication overhead, coordinating EVs only at sensitive nodes (those with a higher VUF value) is recommended to decrease the computational burden and communication overhead; and

iv) it is recommended that three-phase four-leg EV converters be used to compensate for the neutral current along with other ancillary services such as active and reactive power support to the grid.

Though it is evident from the obtained results that the proposed hierarchical control strategy mitigates voltage unbalance and neutral current, this study does not consider individual EV users' driving mileage and time-varying energy cost. However, this will be considered in future work to achieve a win-win solution between grid operators and EV users.

ACKNOWLEDGEMENT

The authors would like to thank ENERGEX for providing the distribution grid model for research. This research is supported by an Australian Government Research Training Program.

REFERENCES

[1] T. Tanabe, T. Funabashi, K. Nara, Y. Mishima, and R. Yokoyama, "A loss minimum re-configuration algorithm of distribution systems under three-phase unbalanced condition," in Proc. *2008 IEEE Electrical Power and Energy Conference (EPEC)*, pp. 1-4, 20-24 July. 2008, Pittsburgh, Pennsylvania, USA.

[2] K. H. Chua, J. Wong, Y. S. Lim, P. Taylor, E. Morris, and S. Morris, "Mitigation of voltage unbalance in low voltage distribution network with high level of photovoltaic system," in *Energy Procedia*, vol. 12, pp. 495–501, 2011.

[3] H. a. K. Golmohamadi, Reza, "Application of robust optimization approach to determine optimal retail electricity price in presence of intermittent and conventional distributed generation considering demand response,"*J. Control, Automation and Elec. Systems.*, vol. 28, pp. 664-678, Dec. 2017.

[4] F. J. Ruiz-Rodriguez, J. C. Hernández, and F. Jurado, "Voltage unbalance assessment in secondary radial distribution networks with single-phase photovoltaic systems," *Int. J. Elec. Power Energy Sys.*, vol. 64, pp. 646-654, Jan. 2015.

[5] A. Rodriguez-Calvo, R. Cossent, and P. Frías, "Integration of PV and EVs in unbalanced residential LV networks and implications for the smart grid and advanced metering infrastructure deployment," *Int. J. Elec. Power Energy Sys.*, vol. 91, no. Sup. C, pp. 121-134, Oct. 2017.

[6] A. Siddique, G. S. Yadava, and B. Singh, "Effects of voltage unbalance on induction motors," in Conference Record of *IEEE International Symposium on Electrical Insulation*, pp. 26–29, 2004.

[7] D. Sreenivasarao, P. Agarwal, and B. Das, "Neutral current compensation in three-phase, four-wire systems: a review," *Electric Power Systems Res.*, vol. 86, pp. 170-180, May. 2012.

[8] M. R. Islam, H. Lu, M. J. Hossain, and L. Li, "Mitigating unbalance using distributed network reconfiguration techniques in distributed power generation grids with services for electric vehicles: a review," *J. Cleaner Prod.*, vol. 239, pp. 910-932, Dec. 2019.

[9] M. R. Islam, H. H. Lu, M. J. Hossain, and L. Li, "Compensating neutral current, voltage unbalance and improving voltage of an unbalanced distribution grid connected with EV and renewable energy sources," in *2019 22nd International Conference on Electrical Machines and Systems, ICEMS 2019*, pp. 1-5, 2019.

[10] F. Shahnia, P. J. Wolfs, and A. Ghosh, "Voltage unbalance reduction in low voltage feeders by dynamic switching of residential customers among three phases," *IEEE Trans. Smart Grid*, vol. 5, no. 3, pp. 1318–1327, 2014.

[11] H. F. Farahani, "Improving voltage unbalance of low-voltage distribution networks using plug-in electric vehicles," *J. Cleaner Prod.*, vol. 239, pp. 336-346, Apr. 2017.

[12] F. Shahnia, A. Ghosh, G. Ledwich, and F. Zare, "Voltage unbalance improvement in low voltage residential feeders with rooftop PVs using custom power devices," *Int. J. Electr. Power Energy Syst.*, vol. 55, pp. 362–377, Feb. 2014.

[13] N. Jabalameli, X. Su, and A. Ghosh, "Online centralized charging coordination of pevs with decentralized var discharging for mitigation of voltage unbalance," *IEEE Power Energy Technol. Syst. J.*, vol. 6, no. 3, pp. 152–161, Aug. 2019.

[14] K. Knezović and M. Marinelli, "Phase-wise enhanced voltage support from electric vehicles in a Danish low-voltage distribution grid," *Electr. Power Syst. Res.*, vol. 140, pp. 274–283, Nov. 2016.

[15] S. Weckx and J. Driesen, "Load balancing with ev chargers and pv inverters in unbalanced distribution grids," *IEEE Trans. Sustain. Energy*, vol. 6, no. 2, pp. 635–643, Apr. 2015.

[16] Yazdani and R. Iravani, "A unified dynamic model and control for the voltage-sourced converter under unbalanced grid conditions," in Proc. *2006 IEEE Power Engineering Society General Meeting*, pp.1620-1629, 18-22 June 2006, Montreal, Que., Canada.

[17] P. T. Cheng, C. A. Chen, T. L. Lee, and S. Y. Kuo, "A cooperative imbalance compensation method for distributed-generation interface converters," *IEEE Trans. Ind. Appl.*, vol. 45, no. 2, pp. 805–815, 2009.

[18] Meersman, B. Renders, L. Degroote, T. Vandoorn, and L. Vandevelde, "Three-phase inverter-connected DG-units and voltage unbalance," *Electr. Power Syst. Res.*, vol. 81, no. 4, pp. 899–906, Apr. 2011.

[19] M. J. Hossain, F. H. M. Rafi, G. Town, and J. Lu, " A multifunctional three-Phase four-Leg PV-SVSI with dynamic capacity distribution method," *IEEE Trans. Ind. Informatics*, vol. 14, no. 6, pp. 2507–2520, Jun. 2018.

[20] E. Demirok, D. Sera, R. Teodorescu, P. Rodriguez, and U. Borup, "Clustered PV inverters in LV networks: An overview of impacts and comparison of voltage control strategies," in Proc. *2009 IEEE Electrical Power and Energy Conference (EPEC)*, pp. 1-6, 22-23 Oct. 2009, Montreal, Que., Canada.

[21] M. M. Far, E. Pashajavid, and A. Ghosh, "Power capacity management of dynamic voltage restorers used for voltage sag and unbalance compensation," in Proc. *2017 Australasian Universities Power Engineering Conference (AUPEC)*, pp. 1-6, Melbourne, Australia, 19-22 November, 2017.

[22] IEEE recommended practice for monitoring electric power quality, *IEEE standard 1159*, 2009.

[23] L. Fortescue, "Polyphase power representation by means of symmetrical coordinates," *Trans. of the American Institute of Elec. Engineers*, vol. XXXIX, no. 2, pp. 1481-1484, 1920.

[24] "Communication networks and systems for power utility automation – part 5: Communication requirements for functions and device models," IEC Standard 61850-5:2013, 2013.

[25] M. R. Islam, H. Lu, *et al*., "Optimal dispatch of electrical vehicle and PV power to improve the power quality of an unbalanced distribution grid," in Proc. *2019 Int. Conf. High Perfo. Big Data and Int. Sys. (HPBD&IS)*, pp. 258-263, 9-11 May 2019, Shenzhen, China.

[26] F. H. M. Rafi, M. J. Hossain, and J. Lu, "Improved neutral current compensation with a four-leg PV smart VSI in a LV residential network," *IEEE Trans. Power Del.*, vol. 32, no. 5, pp. 2291-2302, 2017.

[27] G. Germany, "*DIgSILENT Powerfactory Software Package*". Available online: https://www. digsilent.de.

[28] N. Z. Xu and C. Y. Chung, "Uncertainties of EV charging and effects on well-being analysis of generating systems," *IEEE Trans. Power Sys*., vol. 30, no. 5, pp. 2547-2557, 2015.

[29] M. Erol-Kantarci and H. T. Mouftah, "Supply and load management for the smart distribution grid using wireless networks," in Proc. *2012 Japan-Egypt Conference on Electronics, Communications and Computers*, pp. 145-150, 6-9 March 2012, Alexendaria, Egypt.

[30] M. Esmaili and A. Goldoust, "Multi-objective optimal charging of plug-in electric vehicles in unbalanced distribution networks," *Int. J. of Elec. Power and Energy sys*., vol. 73, pp. 644-652, Dec, 2015.